scientific reports

Check for updates

OPEN

CGJO: a novel complex-valued encoding golden jackal optimization

Jinzhong Zhang, Gang Zhang✉, Min Kong, Tan Zhang & Duansong Wang

Golden jackal optimization (GJO) is inspired by mundane characteristics and collaborative hunting behaviour, which mimics foraging, trespassing and encompassing, and capturing prey to refresh a jackal's position. However, the GJO has several limitations, such as a slow convergence rate, low computational accuracy, premature convergence, poor solution efficiency, and weak exploration and exploitation. To enhance the global detection ability and solution accuracy, this paper proposes a novel complex-valued encoding golden jackal optimization (CGJO) to achieve function optimization and engineering design. The complex-valued encoding strategy deploys a dual-diploid organization to encode the real and imaginary portions of the golden jackal and converts the dual-dimensional encoding region to the single-dimensional manifestation region, which increases population diversity, restricts search stagnation, expands the exploration area, promotes information exchange, fosters collaboration efficiency and improves convergence accuracy. CGJO not only exhibits strong adaptability and robustness to achieve supplementary advantages and enhance optimization efficiency but also balances global exploration and local exploitation to promote computational precision and determine the best solution. The CEC 2022 test suite and six real-world engineering designs are utilized to evaluate the effectiveness and feasibility of CGJO. CGJO is compared with three categories of existing optimization algorithms: (1) WO, HO, NRBO and BKA are recently published algorithms; (2) SCSO, GJO, RGJO and SGJO are highly cited algorithms; and (3) L-SHADE, LSHADE-EpsSin and CMA-ES are highly performing algorithms. The experimental results reveal that the effectiveness and feasibility of CGJO are superior to those of other algorithms. The CGJO has strong superiority and reliability to achieve a quicker convergence rate, greater computation precision, and greater stability and robustness.

Keywords Golden jackal optimization, Complex-valued encoding, Global exploration, Local exploitation, Experimental results

The primary intention of optimal operation is to fulfil certain decision constraints and identify the optimal implementation. When solving some large-scale and complex combinational optimization issues, conventional techniques present inherent weaknesses, such as low computational productivity, poor optimization precision, premature convergence, exponentially increasing time and combinatorial explosion. However, evolutionary algorithms not only have simple framework operations, good parallelism, strong robustness, easy expansion, strong self-organization, high calculation accuracy and strong stability but can also effectively realize complementary advantages between algorithms or optimization strategies to acquire accurate global values. Some evolutionary algorithms include the walrus optimizer (WO)[1], hippopotamus optimization (HO)[2], sand cat swarm optimization (SCSO)[3], Newton−Raphson-based optimizer (NRBO)[4], black-winged kite algorithm (BKA)[5], linear population size reduction-success-history adaptation for differential evolution (L-SHADE)[6], ensemble sinusoidal incorporated with L-SHADE (LSHADE-EpSin)[7], covariance matrix adaptation evolution strategy (CMA-ES)[8], and golden jackal optimization (GJO)[9].

Mohapatra et al. utilized a modified GJO to accomplish the functions and engineering designs; this methodology exhibited remarkable reliability and dependability in delivering the solution[10]. Zhang et al. introduced an enhanced GJO to accomplish an infinite impulse response network; this methodology achieved greater computational efficiency and greater recognition precision[11]. Zhang et al. designed a revised GJO to segment images,

School of Electrical and Photoelectronic Engineering, West Anhui University, Lu'an 237012, China. ✉email: zhanggang@wxc.edu.cn

and this methodology displayed good robustness and adaptability to prevent search stagnation and increase segmentation quality[12]. Hanafi et al. integrated a binary GJO to accomplish intrusion detection in the Internet of Things; this methodology achieved excellent superiority and practically acquired the maximum percentage accuracy and the finest detection effect[13]. Ghandourah et al. created a GJO to anticipate the thermal properties of solar stills; this methodology deployed extensive investigation and extraction to transmit a higher prediction accuracy and faster calculation efficiency[14]. Wang et al. mentioned a reinforced GJO to segment COVID-19 images; this methodology revealed good durability and feasibility in promoting the computation rate and segmentation precision[15]. Das et al. deployed the GJO to predict feature selection of software failure; this methodology has substantial relevance and dependability to achieve high classification precision and optimization efficiency[16]. Snášel et al. introduced an elite-opposition GJO to accomplish multiobjective engineering issues; this methodology exhibited certain superiority and resiliency in generating globally accurate values [17]. Housein et al. devised a modified GJO to segment skin cancer images; this methodology has strong feasibility and practicality[18]. Zhang et al. utilized binary GJO with a stochastic canvas map and cosine resemblance for selecting features, and this methodology demonstrated substantial superiority in terms of the convergence rate and calculation accuracy[19]. Lu et al. proposed a refined GJO and random configuration network to accomplish fault diagnosis of power transformers; this methodology provided excellent reliability and exploitation to increase the optimization accuracy and calculation efficiency[20]. Nanda et al. utilized an altered GJO based on a sine cosine and adopted a scaling factor to design an adaptive fuzzy PIDF controller; this methodology showed significant robustness and superiority to create better control parameters[21]. Wang et al. provided an adaptive GJO to identify abnormal user behaviour; this methodology exhibited great dependability and superiority in achieving the optimal parameters and the best actual value[22]. Yang et al. mentioned an upgraded GJO to achieve the finest distribution of parking locations for wine turbines and electric automobiles; this methodology had excellent predictability for decreasing grid energy losses and minimizing the objective value[23]. Najjar et al. combined GJO with a long short-term model to forecast the tribological properties of alumina-coated alumina; this methodology exhibited exceptional durability and superiority to acquire the ideal optimization solution[24]. Mahdy et al. utilized the GJO to design an integrated wave electricity and photovoltaic system supplying turbocharging stations; this methodology displayed good reliability and stability to mimic and maximize the issue[25]. Wang et al. described a customized GJO to segment aerial images; this methodology exhibited extensive investigation and exploitation to generate a greater computation rate and superior segmentation quality[26]. Wang et al. mentioned multistrategy GJO to accomplish function optimization and engineering design; this methodology exhibited strong global detection ability to avoid search stagnation and determine the best solution[27]. Zhang et al. deployed GJO with a lateral inhibition strategy to accomplish image matching; this methodology has strong reliability and dependability to achieve an accurate registration rate and superior exploration accuracy[28]. Sundar Ganesh et al. released a modified GJO to accomplish photovoltaic parameter estimation; this methodology utilized exploration and exploitation to increase computational efficiency and determine the optimal parameter[29]. Bai et al. constructed an enhanced GJO to accomplish function optimization and engineering design; this methodology exhibited remarkable superiority and reliability in efficiently completing a global search and achieved the best convergence accuracy[30]. Zhong et al. delivered a multiobjective GJO to resolve dynamic economic emission dispatch; this methodology featured strong superiority and robustness to complete the optimal scheduling solution[31]. Elhoseny et al. implemented a modified multistrategy GJO to accomplish function optimization and engineering design; this methodology exhibited strong adaptability and robustness to increase the solution efficiency and convergence accuracy[32]. Alharthi et al. introduced a modified GJO with chaotic maps to accomplish chemical data classification; this methodology exhibited superior evaluation efficiency and classification accuracy[33]. Li et al. integrated a cross-mutation GJO to accomplish function optimization and engineering design; this methodology exhibited strong effectiveness and feasibility to achieve a quicker convergence rate and greater computational precision[34]. In summary, research on the GJO has focused mainly on algorithm improvement and application. (1) The modified GJO uses efficient exploration strategies, effective encoding forms or hybrid optimization methods to realize supplementary advantages and enhance the optimization efficiency, which are applied to achieve function optimization and engineering design. These modified algorithms can effectively avoid search stagnation and promote solution efficiency, which balances exploration and exploitation to improve the convergence speed and calculation accuracy. (2) The modified GJO exhibits strong stability, robustness, feasibility, scalability, and parallelism to solve various large-scale and complex frontier problems, such as artificial intelligence, systems control, pattern recognition, engineering technology and network communication. The modified GJO method exhibits strong adaptability and robustness to promote computational precision and determine the best solution.

Although the above modified versions of the original GJO have enhanced the convergence speed and calculation accuracy to a certain extent, they still cannot efficiently achieve a balance between global exploration and local exploitation to avoid search stagnation and determine the best solution. The no-free-lunch (NFL) theorem states that there is no specific optimization algorithm that can resolve all optimization issues. More advanced and superior algorithms will continue to emerge in the improvement and application of the GJO, which motivates us to establish a novel CGJO for function optimization and engineering design. The complex-valued encoding mechanism is introduced into the basic GJO to encode the real and imaginary portions of the golden jackal and renew the position information, which increases population diversity, restricts search stagnation, expands the exploration area, promotes information exchange, fosters collaboration efficiency and improves convergence accuracy. The main contributions can be summarized as follows: (1) Complex-valued encoding golden jackal optimization (CGJO) is proposed to resolve the global optimization problem. (2) The complex-valued encoding mechanism increases population diversity, restricts search stagnation, expands the exploration area, promotes information exchange, fosters collaboration efficiency and improves convergence accuracy. (3) CGJO is compared with various optimization algorithms, including recently published, highly cited, and highly performing algorithms. (4) CGJO is tested against the CEC 2022 test suite and six real-world engineering designs by performing

simulation experiments and analysing the results. (5) CGJO exhibits strong effectiveness and feasibility and outperforms the other algorithms.

The remainder of this article is divided into the following sections. Section "Golden jackal optimization" reveals the GJO. Section "Complex-valued encoding golden jackal optimization" describes the CGJO. Section "Simulation evaluation and result analysis" proposes comparative experiments and result analysis. Section "CGJO for engineering design" introduces the comparative experiments and result analysis. Section "Conclusions and future research" summarizes the findings, research limitations, and recommendations for future research.

Golden jackal optimization

The jackal collaborative hunting procedure is depicted in Fig. 1.

Search domain

In GJO, the search agent is distributed arbitrarily, and the jackal population is initialized arbitrarily. The initial search agent is established as:

$$Y_0 = Y_{\min} + rand(Y_{\max} - Y_{\min}) \tag{1}$$

where Y_0 represents the initial population location of the golden jackal, $rand \in [0, 1][0, 1]$, $Y_{\min}$ and $Y_{\max}$ represent the lower and upper boundaries, respectively.

The optimal and suboptimal search agent portrays a jackal pair, and the prey matrix is established as:

$$Prey = \begin{bmatrix} Y_{1,1} & Y_{1,2} & \cdots & Y_{1,d} \\ Y_{2,1} & Y_{2,2} & \cdots & Y_{2,d} \\ \vdots & \vdots & \vdots & \vdots \\ Y_{n,1} & Y_{n,2} & \cdots & Y_{n,d} \end{bmatrix} \tag{2}$$

where $Y_{i,j}$ represents the *jth* dimension of the *ith* prey, n represents the prey size, and d represents the question dimension. The fitness matrix F_{OA} is established as:

$$F_{OA} = \begin{bmatrix} f(Y_{1,1};\, Y_{1,2};\, Y_{1,d}) \\ f(Y_{2,1};\, Y_{2,2};\, Y_{2,d}) \\ \vdots \\ f(Y_{n,1};\, Y_{n,2};\, Y_{n,d}) \end{bmatrix} \tag{3}$$

where f portrays the fitness function. The jackal pair renews and captures the prey according to the corresponding prey position.

Foraging the prey (exploration)

Jackals utilize their distinctive predatory abilities to perceive, track and capture prey; however, the target occasionally cannot be caught quickly and escapes. Hence, the male jackal leads the female jackal to search for prey, thereby facilitatig a more efficient the hunting process. The positions are established as:

$$Y_1(t) = Y_M(t) - E \cdot \left| Y_M(t) - rl \cdot Prey(t) \right| \tag{4}$$

$$Y_2(t) = Y_{FM}(t) - E \cdot \left| Y_{FM}(t) - rl \cdot Prey(t) \right| \tag{5}$$

where t represents the current iteration, $Prey(t)$ represents the prey location, $Y_M(t)$ and $Y_{FM}(t)$ represent the locations of the male and female jackals, and $Y_1(t)$ and $Y_2(t)$ represent the renewed locations of the male and female jackals, respectively.

The prey's energy to avoid E is established as:

$$E = E_1 \cdot E_0 \tag{6}$$

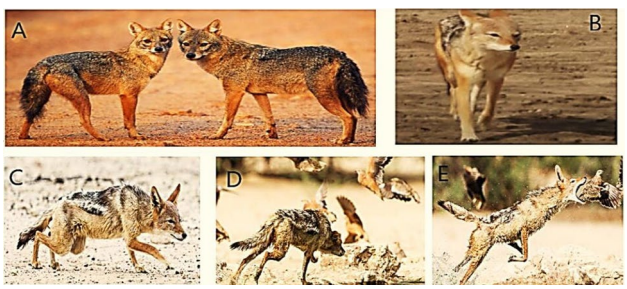

Fig. 1. (**A**) Pair of golden jackals; (**B**) Foraging prey; (**C**) Trespassing and encircling prey; (**D**,**E**) Trapping prey.

where E_1 represents the energy of the prey, and E_0 represents the initial energy of the prey.

$$E_0 = 2 \cdot r - 1 \tag{7}$$

where r is a stochastic value in [0,1].

$$E_1 = c_1 \cdot (1 - (t / T)) \tag{8}$$

where T represents the maximum number of iterations, $c_1 = 1.5$, and E_1 linearly decreases from 1.5 to 0.

The stochastic value rl based on the Levy distribution is established as:

$$rl = 0.05 \cdot LF(y) \tag{9}$$

The Levy flight LF portrays the fitness function.

$$LF(y) = 0.01 \times (\mu \times \sigma) / (\left| v^{(1/\beta)} \right|); \quad \sigma = \left(\frac{\Gamma(1+\beta) \times \sin(\pi\beta/2)}{\Gamma\left(\frac{1+\beta}{2}\right) \times \beta \times \left(2^{\frac{\beta-1}{2}}\right)} \right)^{1/\beta} \tag{10}$$

where μ and v portray stochastic values in (0,1), $\beta = 1.5$.

The jackal pair's renewed position is established as:

$$Y(t+1) = \frac{Y_1(t) + Y_2(t)}{2} \tag{11}$$

Encircling and trapping the prey (exploitation)

The jackal can pounce, surround and devour the prey. The positions are established as follows:

$$Y_1(t) = Y_M(t) - E \cdot \left| rl \cdot Y_M(t) - Prey(t) \right| \tag{12}$$

$$Y_2(t) = Y_{FM}(t) - E \cdot \left| rl \cdot Y_{FM}(t) - Prey(t) \right| \tag{13}$$

where $Prey(t)$ represents the prey location, $Y_M(t)$ and $Y_{FM}(t)$ represent the locations of the male and female jackals, respectively, and $Y_1(t)$ and $Y_2(t)$ represent the renewed locations of the male and female jackals, respectively. The renewed location is established as Eq. (11).

The pseudocode of GJO is listed in Algorithm 1.

Begin

Step 1. Initialize the stochastic jackal population $Y_i(i = 1, 2, ..., n)$

Step 2. Estimate the fitness value of each jackal

$Y_1 =$ best prey (male jackal position)

$Y_2 =$ second best prey (female jackal position)

Step 3. while ($t < T$) do

for each jackal

Alter the avoiding energy E via Eqs. (6), (7) and (8)

Alter the stochastic value rl via Eqs. (9) and (10)

if $(|E| \geq 1)$

Alter the jackal position via Eqs. (4), (5) and (11)

else $(|E| < 1)$

Alter the jackal position via Eqs. (12), (13) and (11)

end if

end for

Ascertain and regulate the boundary if the jackal exceeds the search domain

Estimate the fitness value of each jackal

Alter Y_1 if there is a superior position

$t = t + 1$

end while

Restore Y_1

End

Algorithm 1. GJO.

Complex-valued encoding golden jackal optimization

In natural ecosystems, chromosomes of sophisticated cellular structures are regularly composed of double or multiple strands. Complex-valued encoding uses mainly diploid technology to describe one allele of a chromosome and alter its position independently of the real and imaginary portions. This technology can enhance algorithmic parallelism, tap population diversity, avoid premature convergence, expand the feature space, improve the search efficiency and increase the information capacity. For an issue with M distinct factors, the structure is established as[35,36]:

$$Y_p = R_p + iI_p, \quad p = 1, 2, 3, ..., M \tag{14}$$

where (R_P, I_P) represents the gene of an organism with a diploid structure and R_P and I_P represent the real and imaginary parts of the complex-virtual encoding, respectively. The chromosome structure of the organism is outlined in Table 1.

Initializing the complex-valued encoding population

Assume that the defined span is $[A_k, B_k], k = 1, 2, .., M$, and that stochastics generate M modulus and M arguments.

$$\rho_k \in \left[0, \frac{B_k - A_k}{2}\right], \quad k = 1, 2, ..., M \tag{15}$$

$Gene_1$	$Gene_2$	$Gene_i$	$Gene_M$
(R_{P1}, I_{P1})	(R_{P2}, I_{P2})	...	(R_{PM}, I_{PM})

Table 1. Chromosome model of the organism.

$$\theta_k = [-2\pi, 2\pi], \quad k = 1, 2, ..., M \tag{16}$$

The M complex values are established as:

$$Y_{Rk} + iY_{Ik} = \rho_k(\cos\theta_k + i\sin\theta_k), \quad k = 1, 2, ..., M \tag{17}$$

The GJO uses M real and imaginary parts to alter the jackal location.

The altering methodology of CGJO

Foraging prey

(1)(1) Alter the real portions:

$$Y_{1R}(t) = Y_{MR}(t) - E \cdot \left|Y_{MR}(t) - rl \cdot Prey_R(t)\right| \tag{18}$$

$$Y_{2R}(t) = Y_{FMR}(t) - E \cdot \left|Y_{FMR}(t) - rl \cdot Prey_R(t)\right| \tag{19}$$

$$Y_R(t+1) = \frac{Y_{1R}(t) + Y_{2R}(t)}{2} \tag{20}$$

(1)(1) Alter the imaginary portions:

$$Y_{1I}(t) = Y_{MI}(t) - E \cdot \left|Y_{MI}(t) - rl \cdot Prey_I(t)\right| \tag{21}$$

$$Y_{2I}(t) = Y_{FMI}(t) - E \cdot \left|Y_{FMI}(t) - rl \cdot Prey_I(t)\right| \tag{22}$$

$$Y_I(t+1) = \frac{Y_{1I}(t) + Y_{2I}(t)}{2} \tag{23}$$

Encircling and trapping prey

(1)(1) Alter the real portions:

$$Y_{1R}(t) = Y_{MR}(t) - E \cdot \left|rl \cdot Y_{MR}(t) - Prey_R(t)\right| \tag{24}$$

$$Y_{2R}(t) = Y_{FMR}(t) - E \cdot \left|rl \cdot Y_{FMR}(t) - Prey_R(t)\right| \tag{25}$$

$$Y_R(t+1) = \frac{Y_{1R}(t) + Y_{2R}(t)}{2} \tag{26}$$

(1)(1) Alter the imaginary portions:

$$Y_{1I}(t) = Y_{MI}(t) - E \cdot \left|rl \cdot Y_{MI}(t) - Prey_I(t)\right| \tag{27}$$

$$Y_{2I}(t) = Y_{FMI}(t) - E \cdot \left|rl \cdot Y_{FMI}(t) - Prey_I(t)\right| \tag{28}$$

$$Y_I(t+1) = \frac{Y_{1I}(t) + Y_{2I}(t)}{2} \tag{29}$$

where $Prey_R$ and $Prey_I$ indicate the real and imaginary portions of the prey, respectively. Y_R and Y_I indicate the real and imaginary portions of the golden jackal, respectively.

The methodology for computing the fitness value

The fitness value of the complex value is established as:

$$\rho_k = \sqrt{Y_{Rk}^2 + Y_{Ik}^2}, \quad k = 1, 2, ..., M \tag{30}$$

$$Y_k = \rho_k \mathrm{sgn}\left(\sin\left(\frac{Y_{Ik}}{\rho_k}\right)\right) + \frac{B_k + A_k}{2}, \quad k = 1, 2, ..., M \tag{31}$$

where Y_k represents the converted authentic variable.

The solution procedure of CGJO

The CGJO increases the population diversity, improves algorithmic parallelism, accelerates global exploration and promotes optimization. The pseudocode of CGJO is listed in Algorithm 2. The flowchart of the CGJO is shown in Fig. 2.

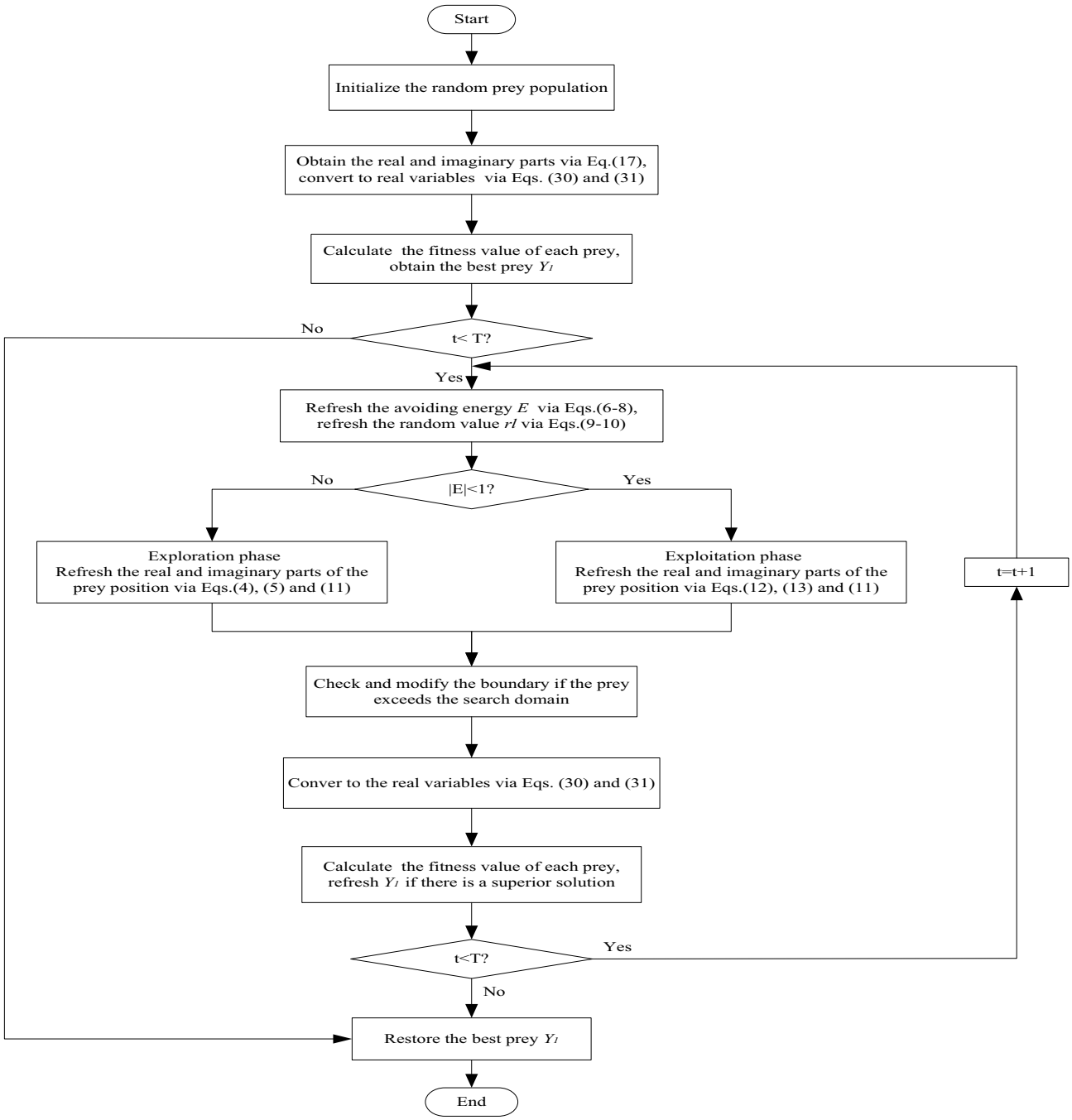

Fig. 2. Flowchart of the CGJO.

Begin

Step 1. Initialize the stochastic jackal population $Y_i(i=1,2,...,n)$: $\rho_k \in \left[0, \frac{B_k - A_k}{2}\right]$ and $\theta_k = [-2\pi, 2\pi]$, obtain the real and imaginary parts via Eq. (17), and convert them to real variables via Eqs. (30) and (31)

Step 2. Estimate the fitness value of each jackal

$Y_1 =$ best prey (male jackal position)

$Y_2 =$ second best prey (female jackal position)

Step 3. while ($t < T$) do

for each jackal

Alter the avoiding energy E via Eqs. (6), (7) and (8)

Alter the stochastic value rl via Eqs. (9) and (10)

if $(|E| \geq 1)$

Alter the real and imaginary parts of the jackal position via Eqs. (4), (5) and (11)

else $(|E| < 1)$

Alter the real and imaginary parts of the jackal position via Eqs. (12), (13) and (11)

end if

end for

Ascertain and regulate the boundary if the jackal exceeds the search domain

Conver to the real variables via Eqs. (30) and (31)

Estimate the fitness value of each jackal

Alter Y_1 if there is a superior position

$t = t + 1$

end while

Restore Y_1

End

Algorithm 2. CGJO.

Computational complexity of the CGJO

Time complexity The time complexity is established to estimate the amount of resources consumed when each algorithm operates independently, which directly relates the question's operational scale to the computational time. The big-O notation is a practical methodology for demonstrating the algorithm's directness and dependability. The CGJO contains three primary processes: initialization, estimation of the fitness function, and alteration of the jackal position. In CGJO, n represents the population size, T represents the maximum number of iterations, and d represents the question dimension. The initialization involves $O(n)$. Each process consists of estimating the fitness function and altering the jackal position $O(T \times n) + O(T \times n \times d)$. Complex-valued encoding enhances algorithmic parallelism, taps population diversity, avoids premature convergence, expands the feature space, improves the search efficiency and increases the information capacity. CGJO exhibits excellent durability and dependability to acquire complementary advantages and regulates exploration and exploitation to promote computational precision. The time complexity of CGJO is $O(n \times (T + T \times d + 1))$.

Space complexity the space complexity is utilized to store the space exhausted by the CGJO. In CGJO, n represents the population size, and d represents the question dimension. CGJO not only exhibits strong adaptability and robustness to achieve supplementary advantages and enhance optimization efficiency but also balances global exploration and local exploitation to promote computational precision and determine the best solution. The space complexity of the CGJO involves $O(n \times d)$.

Simulation evaluation and result analysis

Experimental setup

The mathematical evaluations were performed with Windows 10 with an Intel Core i7-8750H 2.2 GHz CPU, a GTX1060, and 8 GB of memory.

Parameter settings

The algorithm's parameters are a set of distinctive experimental values that are extracted from the original papers.

WO: stochastic value $rand \in [0,1]$, danger factors $A \in [0,2]$, $R \in [-1,1]$, stochastic values $r_{1-5} \in (0,1)$, migration step control factor $\beta \in [0,1]$, distress factor $p \in (0,1)$, standard deviation $\sigma_y = 1$, control value $\alpha = 1.5$, range $\theta \in [0,\pi]$.

HO: stochastic values $r_{1-6} \in (0,1)$, integer $I_{1,2} \in [1,2]$, stochastic value $\omega \in [0,1]$, stochastic value $\nu \in [0,1]$, constant value $\theta = 1.5$.

SCSO: constant value $S_M = 2$, sensitivity range $r_G \in (0,2)$, stochastic value $rand \in [0,1]$, range $\theta \in [0,2\pi]$, stochastic value $R \in [-1,1]$.

NRBO: stochastic value $\delta \in [-1,1]$, stochastic values $a, b \in (0,1)$, stochastic values $r_{1,2} \in (0,1)$, stochastic value $\theta_1 \in (-1,1)$, stochastic value $\theta_2 \in (-0.5,0.5)$.

BKA: stochastic value $rand \in [0,1]$, constant value $p = 0.9$, stochastic value $r \in [0,1]$, Cauchy mutation $C(0,1)$, $\delta = 1$, $\mu = 0$.

L-SHADE: $Pbest = 0.1$, $Arc\ rate = 2$, learning rate $c = 0.8$, threshold max $\_nfes/2$.

LSHADE-EpSin: $Pbest = 0.1$, $Arc\ rate = 2$, learning rate $c = 0.8$, threshold max $\_nfes/2$.

CMA-ES: parent number $\mu = \lfloor \lambda/2 \rfloor$, weight factor $w = \log(mu + 0.5) - \log(1:mu)$, step size $\sigma = 0.3 \times 200$.

GJO: stochastic value $r \in [0,1]$, constant value $c_1 = 1.5$, initial state $E_0 \in [-1,1]$, energy decrease $E_1 \in [0,1.5]$, default factor $\beta = 1.5$, stochastic values $u, v \in (0,1)$.

GJO-based on ranking-based mutation operator (RGJO)[37]: stochastic value $r \in [0,1]$, constant value $c_1 = 1.5$, initial state $E_0 \in [-1,1]$, energy decrease $E_1 \in [0,1.5]$, default factor $\beta = 1.5$, stochastic values $u, v \in (0,1)$, scaling factor $F = 0.7$.

GJO-based on the simplex method (SGJO)[38]: stochastic value $r \in [0,1]$, constant value $c_1 = 1.5$, initial state $E_0 \in [-1,1]$, energy decrease $E_1 \in [0,1.5]$, default factor $\beta = 1.5$, stochastic values $u, v \in (0,1)$, stochastic value $k \in (0,1)$, reflectivity $\alpha = 1$, expansion factor $\gamma = 1.5$, compression factor $\beta_1 = 0.5$, contraction factor $\beta_2 = 0.2$.

CGJO: stochastic value $r \in [0,1]$, constant value $c_1 = 1.5$, initial state $E_0 \in [-1,1]$, energy decrease $E_1 \in [0,1.5]$, default factor $\beta = 1.5$, stochastic values $u, v \in (0,1)$.

Benchmark functions

CGJO is implemented to accomplish the CEC 2022 benchmark functions[39,40], which confirms its practicality and feasibility. Table 2 outlines the CEC 2022 test suite.

Experimental result analysis

The population size is 50, the maximum number of iterations is 1000, and the number of separate runs is 30. Best, Std, Mean, Median and Worst represent the optimal value, standard deviation, mean value, median value and worst value, respectively[41]. The ranking is based on the standard deviation. The robustness of the optimizaiton algorithms is to maintain the stable ability in term of noise and outliers. For noise in data sets, the optimization algorithms utilize the following strategies: (1) gradient smoothing, (2) momentum method, (3) adaptive learning optimizer, (4) smooth optimization objective function, (5) robust loss function. For outliers in data sets, the optimization algorithms utilize the following strategies: (1) delete outliers, (2) replace outliers, (3) convert outliers.

The simulation results of different algorithms for the CEC 2022 test functions are outlined in Table 3. For F1 and F2, compared with those of the basic GJO, the optimal values, standard deviations, mean values, median values and worst values of RGJO, SGJO and CGJO are significantly greater. The CGJO method is superior and reliable for identifying the ideal global value. The various evaluation indicators and computational solutions of

Function type	No.	Name	*Dim*	[*lb*,*ub*]	F_{min}
Unimodal function	F1	Shifted and full rotated Zakharov function	10	[−100, 100]	300
Basic functions	F2	Shifted and full rotated Rosenbrock's function	10	[−100, 100]	400
	F3	Shifted and full rotated expanded Schaffer's F_6 function	10	[−100, 100]	600
	F4	Shifted and full rotated non-continuous Rastrigin's function	10	[−100, 100]	800
	F5	Shifted and rotated Levy function	10	[−100, 100]	900
Hybrid functions	F6	Hybrid function 1 ($N = 3$)	10	[−100, 100]	1800
	F7	Hybrid function 2 ($N = 6$)	10	[−100, 100]	2000
	F8	Hybrid function 3 ($N = 5$)	10	[−100, 100]	2200
Composite functions	F9	Composite function 1 ($N = 5$)	10	[−100, 100]	2300
	F10	Composite function 2 ($N = 4$)	10	[−100, 100]	2400
	F11	Composite function 3 ($N = 5$)	10	[−100, 100]	2600
	F12	Composite function 4 ($N = 6$)	10	[−100, 100]	2700

Table 2. Description of CEC2022 test suite.

Function	Result	WO	HO	SCSO	NRBO	BKA	L-SHADE	LSHADE-EpSin	CMA-ES	GJO	RGJO	SGJO	CGJO
F1	Best	300.2130	309.0403	333.8662	396.4065	300.0094	300.0152	300.0000	302.1946	453.9769	338.3932	386.9419	300.0000
	Std	2.094482	63.68451	984.8224	192.7886	1.401565	105.4176	25.71657	54.86285	1947.696	924.0128	1496.385	0.000215
	Mean	301.7536	392.7228	993.1696	691.5273	300.5281	325.1675	311.4229	375.5500	2563.964	931.5736	1948.520	300.0001
	Median	300.8786	381.6787	487.1169	654.6331	300.1015	300.8597	300.0000	365.5108	2807.546	472.5906	1805.048	300.0000
	Worst	308.5147	569.9658	4181.704	1230.933	306.5481	878.5424	421.8946	456.1776	6465.073	2987.586	4589.390	300.0010
	Rank	3	6	10	8	2	7	4	5	12	9	11	1
F2	Best	400.5629	400.0001	400.2925	405.9872	400.0035	400.0074	404.1600	400.0142	404.7350	406.6700	402.3776	400.0000
	Std	25.35779	31.68464	29.22815	25.47904	22.22227	27.20730	24.31578	24.15667	33.54314	15.96363	21.56903	2.000642
	Mean	418.2928	426.3870	429.0072	434.6420	412.8991	418.5663	417.0360	415.5301	440.2734	417.1255	430.6919	400.7227
	Median	408.9161	408.9477	412.2485	422.1621	404.0980	407.8979	408.9161	405.5960	435.8737	411.1550	431.8252	400.0000
	Worst	480.7356	495.8649	495.8306	482.5962	470.7846	475.8162	493.0350	472.6120	575.3141	462.2972	471.6199	408.9162
	Rank	7	11	10	8	4	9	6	5	12	2	3	1
F3	Best	600.0140	602.1127	602.1440	609.0012	602.8699	600.0000	600.0040	600.3814	600.5514	600.1314	600.8426	600.0000
	Std	0.457946	10.27817	9.795200	6.434381	9.824822	9.131703	6.450363	9.146592	5.000873	3.383262	6.821077	0.445899
	Mean	600.3644	622.2184	614.8414	620.6831	622.0874	604.2571	606.4856	615.2597	606.3282	602.5358	610.0306	600.2296
	Median	600.1908	622.1951	613.3532	620.9781	622.7726	601.0723	604.0961	614.8622	605.6116	601.9710	608.7197	600.0003
	Worst	601.4496	646.9043	633.1736	635.0505	642.2783	645.4015	626.1610	635.6286	624.6561	617.7707	631.5368	601.4292
	Rank	2	12	10	5	11	8	6	9	4	3	7	1
F4	Best	810.9445	805.9699	808.9784	811.0988	805.9814	813.9294	806.9647	806.0095	813.3037	806.8717	807.8969	801.9899
	Std	14.04259	5.396266	7.784118	7.323493	6.687331	4.306356	12.78127	5.813394	7.901317	9.905784	7.372880	2.855758
	Mean	836.1125	817.0386	827.1662	823.8555	816.1229	830.9425	828.7686	817.2325	825.2856	823.2192	820.0838	805.5197
	Median	842.4192	817.9093	826.2285	822.9933	815.4265	832.8336	827.7392	817.9326	823.6994	822.4298	820.5300	804.9748
	Worst	857.8684	822.8844	851.0162	841.6521	831.5766	834.5938	853.7272	828.4747	845.2458	840.7523	836.6837	814.1466
	Rank	12	3	8	6	5	2	11	4	9	10	7	1
F5	Best	900.0004	905.0733	902.3788	915.1520	919.6402	900.0001	900.0895	904.0899	900.1978	900.7320	900.8247	900.0000
	Std	7.715744	122.7705	144.5363	91.92995	99.29072	173.7207	66.81567	96.53977	52.21143	26.49567	103.4000	0.501842
	Mean	905.4919	1072.338	1040.274	1031.534	1051.707	973.6975	930.2084	1008.645	949.9401	928.3395	972.0397	900.2903
	Median	902.2257	1049.968	990.4654	1005.998	1029.869	907.1389	912.4313	967.4609	944.1190	921.9169	937.8981	900.0448
	Worst	930.2473	1301.413	1498.419	1267.069	1311.645	1547.236	1260.983	1205.418	1181.579	1011.977	1387.504	901.8173
	Rank	2	10	11	6	8	12	5	7	4	3	9	1
F6	Best	1853.377	1837.090	2256.018	1831.892	1847.444	1892.581	2068.054	1840.095	2699.547	2568.864	1899.819	1801.281
	Std	2094.489	13.31805	1787.439	816.7388	51.14942	2106.705	2259.031	133.1741	3152.739	1966.148	2138.362	6.698119
	Mean	3592.650	1862.297	5009.795	2417.740	1906.827	4550.676	6130.589	1964.579	7805.693	7865.330	6613.351	1808.098
	Median	2537.631	1860.987	4738.463	2054.819	1891.225	4238.307	8008.654	1910.241	8241.257	8478.329	7784.935	1805.246
	Worst	8149.948	1898.149	8161.201	5680.465	2041.014	8075.045	8302.557	2379.799	20197.61	10454.86	8582.073	1827.493
	Rank	8	2	6	5	3	9	11	4	12	7	10	1
F7	Best	2019.814	2025.612	2021.096	2028.559	2009.913	2001.014	2020.051	2011.278	2006.108	2005.136	2019.102	2000.624
	Std	8.935128	14.87673	16.90291	14.13199	17.29082	6.804628	12.53495	10.02943	15.62914	11.48178	16.13403	10.31403
	Mean	2027.167	2045.541	2044.349	2048.825	2034.301	2019.113	2030.410	2029.520	2038.903	2028.652	2040.280	2009.799
	Median	2024.573	2043.629	2043.175	2046.883	2030.952	2020.640	2025.530	2025.512	2037.238	2026.384	2038.803	2004.169
	Worst	2054.966	2099.220	2101.257	2092.758	2087.734	2031.233	2077.322	2048.982	2064.026	2051.679	2073.154	2028.009
	Rank	2	8	11	7	12	1	6	3	9	5	10	4
F8	Best	2200.146	2221.711	2204.057	2215.898	2205.488	2204.057	2202.302	2204.365	2206.531	2221.365	2205.534	2202.540
	Std	7.791932	3.404702	6.758460	37.92741	23.33226	30.85052	7.454976	8.783942	6.394057	2.649609	6.045754	9.436423
	Mean	2221.129	2227.332	2226.092	2241.120	2230.485	2228.670	2221.824	2217.682	2225.710	2225.740	2223.800	2217.860
	Median	2222.120	2227.186	2227.470	2229.764	2226.335	2223.870	2221.856	2222.505	2227.176	2225.818	2225.425	2224.145
	Worst	2237.383	2233.770	2238.416	2357.012	2350.202	2389.572	2231.188	2229.478	2234.448	2231.039	2231.402	2226.252
	Rank	7	2	5	12	10	11	6	8	4	1	3	9
F9	Best	2529.284	2529.296	2529.285	2529.718	2529.284	2529.284	2529.284	2529.285	2529.302	2529.342	2516.820	2529.284
	Std	5.638001	27.88118	38.44790	45.09513	10.80021	26.82598	27.34192	11.00908	37.87201	20.53752	37.16811	0.000480
	Mean	2530.742	2539.096	2573.604	2549.163	2532.186	2534.182	2540.255	2532.885	2590.920	2541.329	2574.247	2529.285
	Median	2529.284	2530.712	2570.678	2532.682	2529.285	2529.284	2529.840	2529.323	2586.795	2530.852	2572.177	2529.284
	Worst	2555.055	2676.217	2676.218	2688.228	2575.421	2676.216	2654.833	2584.141	2661.531	2598.267	2684.591	2529.287
	Rank	2	8	11	12	3	6	7	4	10	5	9	1

Continued

Function	Result	WO	HO	SCSO	NRBO	BKA	L-SHADE	LSHADE-EpSin	CMA-ES	GJO	RGJO	SGJO	CGJO
F10	Best	2500.380	2500.310	2500.243	2500.600	2500.287	2500.300	2500.309	2500.232	2500.264	2500.258	2500.277	2500.129
	Std	53.08442	58.56622	61.74547	65.72414	152.1823	59.28609	55.13067	32.79990	65.03680	49.56434	60.61817	52.26189
	Mean	2529.112	2538.413	2549.923	2584.702	2586.506	2548.008	2533.263	2509.176	2573.219	2524.863	2568.261	2539.432
	Median	2500.667	2500.806	2500.643	2621.824	2557.539	2500.669	2500.842	2500.606	2616.846	2500.475	2611.576	2500.452
	Worst	2655.657	2640.275	2650.202	2660.031	3320.076	2630.024	2641.328	2641.782	2659.347	2645.954	2631.369	2613.195
	Rank	4	6	9	11	12	7	5	1	10	2	8	3
F11	Best	2600.007	2600.266	2601.602	2727.274	2601.056	2600.006	2600.000	2600.868	2725.064	2601.889	2729.011	2600.000
	Std	85.52615	0.131058	112.9647	193.6496	184.4764	133.2479	130.6780	197.0677	231.0027	96.85016	153.7786	95.26248
	Mean	2685.394	2600.488	2754.460	2938.447	2736.044	2800.915	2777.929	2790.890	2975.151	2768.101	2874.727	2868.126
	Median	2750.427	2600.473	2750.678	2817.340	2601.965	2900.019	2751.075	2731.390	2936.940	2750.749	2804.882	2900.000
	Worst	2900.361	2600.791	3000.161	3283.128	3212.722	2912.044	3000.000	3224.199	3393.431	3238.380	3319.115	2920.119
	Rank	2	1	5	10	9	7	6	11	12	4	8	3
F12	Best	2861.405	2859.684	2861.491	2860.832	2859.548	2859.369	2862.709	2862.702	2863.501	2858.654	2853.100	2862.815
	Std	1.125053	16.89455	5.643342	16.75704	2.477016	2.958105	8.720153	1.997828	6.464481	2.260551	7.872567	3.402234
	Mean	2863.880	2873.135	2868.240	2870.974	2864.815	2865.393	2868.651	2865.402	2867.216	2863.594	2859.540	2867.872
	Median	2863.881	2867.464	2866.657	2866.173	2865.214	2865.080	2866.135	2865.167	2865.074	2864.955	2858.464	2867.186
	Worst	2866.662	2946.815	2890.094	2937.095	2873.360	2875.762	2903.422	2871.809	2898.388	2865.937	2898.802	2876.834
	Rank	1	12	7	11	4	5	10	2	8	3	9	6

Table 3. Simulation results of different algorithms for the CEC 2022 test functions.

CGJO are superior to those of WO, HO, SCSO, NRBO, BKA, L-SHADE, LSHADE-EpsSin, CMA-ES, GJO, RGJO and SGJO. CGJO has great computational efficiency and worldwide detection ability to minimize premature convergence and acquire the exact solution. The CGJO portrays tremendous stability and reliability in achieving the optimal ranking. The CGJO can enhance parallelism, tap population diversity and improve optimization efficiency, which uses detection and exploitation to obtain the highest convergence accuracy. For F3 and F5, CGJO not only exhibits obvious superiority and reliability in expanding the optimization space and avoiding search stagnation but also adjusts exploration and exploitation to identify the exact global solutions. The convergence speed and calculation accuracy of the modified GJO are greatly enhanced. The overall optimization ability and evaluation indicators of CGJO are superior to those of WO, HO, SCSO, NRBO, BKA, L-SHADE, LSHADE-EpsSin, CMA-ES, GJO, RGJO and SGJO, and CGJO exhibits strong stability and robustness. The greater minor standard deviation and higher ranking of the CGJO highlight that CGJO delivers good dependability and reliability to satisfy complementary advantages and resolve the function optimization. For F4 and F6, the overall search efficiency and optimization accuracy of RGJO and SGJO are improved compared with those of the basic GJO. CGJO exhibits strong effectiveness and robustness in achieving suboptimal solutions close to the exact solutions. The optimal values, standard deviations, mean values, median values and worst values of CGJO are superior to those of WO, HO, SCSO, NRBO, BKA, L-SHADE, LSHADE-EpsSin, CMA-ES, GJO, RGJO and SGJO. CGJO has better computational accuracy and superior stability. The optimal ranking of CGJO results in good stability and durability. For F7, the standard deviations of CGJO are worse than those of WO, L-SHADE and CMA-ES, but the optimal, mean, median and worst values of CGJO are superior to those of WO, HO, SCSO, NRBO, BKA, L-SHADE, LSHADE-EpsSin, CMA-ES, GJO, RGJO and SGJO. CGJO employs a distinctive encoding methodology to enrich the information capacity and strengthen the detection ability. The ranking of CGJO is slightly lower than those of WO, L-SHADE and CMA-ES. For F8, the various evaluation indicators and computational solutions of CGJO are relatively superior to those of WO, HO, SCSO, NRBO, BKA, L-SHADE, LSHADE-EpsSin, CMA-ES, GJO, RGJO and SGJO. The standard deviation of CGJO is superior to those of L-SHADE, BKA and NRBO but inferior to those of WO, HO, SCSO, LSHADE-EpsSin, CMA-ES, GJO, RGJO and SGJO. For F9, the standard deviations, mean values, median values and worst values of RGJO, SGJO and CGJO are significantly greater than those of the basic GJO. The optimal value of RGJO is worse than that of GJO. The various evaluation indicators and computational solutions of CGJO are superior to those of WO, HO, SCSO, NRBO, BKA, L-SHADE, LSHADE-EpsSin, CMA-ES, GJO, RGJO and SGJO. CGJO employs a distinctive search structure to extend the optimization field and increase the detection efficiency. The ranking of the CGJO is the smallest, and the stability and reliability of this algorithm are better. For F10 and F11, the various evaluation indicators and computational solutions of RGJO, SGJO and CGJO are superior to those of GJO. The optimal values, median values and worst values of CGJO are more substantial than those of WO, HO, SCSO, NRBO, BKA, L-SHADE, LSHADE-EpsSin, CMA-ES, GJO, RGJO and SGJO. The standard deviations, mean values and rankings of CGJO are superior to those of SCSO, NRBO, BKA, L-SHADE, LSHADE-EpsSin, GJO and SGJO. The SCGJO uses the diploid's two-dimensional properties to alter the jackal's position, which not only effectively broadens the exploration area and elevates the population diversity but also inhibits early convergence and realizes the ideal solution. For F12, the optimal values, standard deviations, mean values, median values and worst values of RGJO, SGJO and CGJO are significantly greater than those of the basic GJO. The various evaluation indicators and computational solutions of CGJO are superior to those of HO, SCSO, NRBO, LSHADE-EpsSin, GJO and SGJO. The CGJO has a relatively lower standard deviation and higher ranking. The CGJO uses the combination of the encoding method and GJO to renew the jackal's position, which expands the feature space, enhances

the optimization efficiency and increases the information capacity. CGJO has good stability and durability for identifying the optimal value.

The Wilcoxon rank-sum test is implemented to evaluate whether there is a noticeable discrepancy between CGJO and other methodologies[42,43]. $p < 0.05$ indicates a significant discrepancy, $p \geq 0.05$ indicates no significant discrepancy, and N/A indicates "not applicable". The Wilcoxon signed rank-sum test for CEC 2022 between each algorithm and CGJO is outlined in Table 4.

The convergence graph of each methodology is shown in Fig. 3. The convergence graph can directly and objectively reflect the convergence precision. The CGJO has a good detection capacity and optimization efficiency to accomplish the most effective solution. For the unimodal function F1, CGJO exhibits strong superiority and reliability to avoid premature convergence and achieve the exact solution. The optimal, mean, median and worst values of the CGJO change little. The CGJO has a faster convergence speed and higher calculation accuracy. For basic functions F2, F3, F4 and F5, the various evaluation indicators and computational solutions of the CGJO

Function	CGJO vs										
	WO	HO	SCSO	NRBO	BKA	L-SHADE	LSHADE-EpSin	CMA-ES	GJO	RGJO	SGJO
F1	3.02E−11	3.02E−11	3.02E−11	3.02E−11	3.02E−11	3.02E−11	6.09E−03	3.02E−11	3.02E−11	3.02E−11	3.02E−11
F2	6.12E−10	1.29E−09	9.92E−11	3.69E−11	3.65E−08	3.82E−09	2.53E−10	1.31E−08	4.50E−11	8.99E−11	9.92E−11
F3	8.15E−05	3.02E−11	3.02E−11	3.02E−11	3.02E−11	2.49E−06	1.29E−09	6.07E−11	9.92E−11	6.01E−08	4.98E−11
F4	4.08E−11	5.07E−10	4.08E−11	3.34E−11	1.17E−09	3.28E−11	1.46E−10	3.47E−10	3.34E−11	3.16E−10	1.33E−10
F5	1.34E−07	2.94E−11	2.94E−11	2.94E−11	2.94E−11	1.29E−08	1.34E−08	2.94E−11	1.07E−10	1.30E−10	7.96E−11
F6	3.02E−11	3.02E−11	3.02E−11	3.02E−11	3.02E−11	3.02E−11	3.02E−11	3.02E−11	3.02E−11	3.02E−11	3.02E−11
F7	5.86E−06	4.50E−11	2.61E−10	3.02E−11	2.03E−07	2.61E−02	5.19E−07	6.53E−08	1.56E−08	3.01E−07	7.77E−09
F8	8.07E−05	2.77E−05	1.25E−04	1.31E−08	4.71E−04	2.84E−02	4.38E−02	4.29E−03	1.04E−04	1.24E−03	1.44E−02
F9	9.33E−04	3.02E−11	3.69E−11	3.02E−11	3.83E−05	1.24E−03	1.59E−05	4.50E−11	3.02E−11	3.02E−11	8.48E−09
F10	4.21E−02	6.10E−03	1.03E−02	2.15E−06	3.56E−04	7.96E−03	1.99E−02	5.49E−03	2.84E−04	4.04E−03	1.52E−02
F11	5.60E−07	1.07E−07	1.44E−03	6.52E−04	9.92E−05	9.58E−04	1.87E−06	3.78E−02	2.46E−02	2.32E−06	1.54E−02
F12	6.01E−08	4.64E−02	6.63E−05	1.96E−02	1.32E−04	1.11E−03	2.71E−02	1.06E−03	1.22E−02	1.73E−07	6.72E−10

Table 4. Wilcoxon signed rank-sum test for CEC 2022 between each algorithm and CGJO.

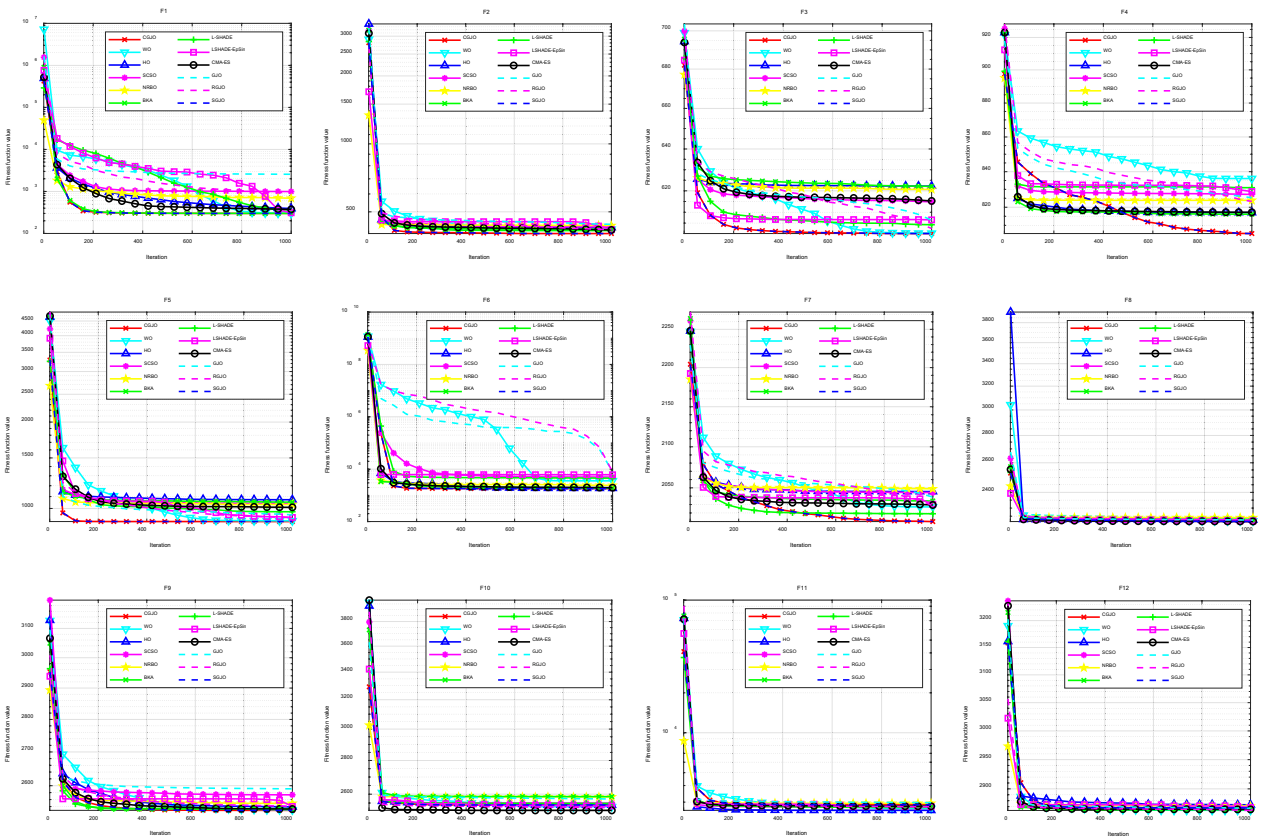

Fig. 3. Convergence graph of each methodology.

are superior to those of the WO, HO, SCSO, NRBO, BKA, L-SHADE, LSHADE-EpsSin, CMA-ES, GJO, RGJO and SGJO, and the particular functions of the CGJO determine the exact global solutions. The CGJO has good stability and durability. The CGJO has better convergence frequency and computational numerical accuracy, which has superiority and reliability to eliminate search stagnation and acquire an appropriate solution. For hybrid functions F6, F7 and F8, compared with those of the basic GJO, the optimal values, standard deviations, mean values, median values and worst values of the CGJO are significantly greater. The various evaluation indicators and computational solutions of the CGJO are superior to those of WO, HO, SCSO, NRBO, BKA, L-SHADE, LSHADE-EpsSin, CMA-ES, GJO, RGJO and SGJO, and CGJO has obvious superiority and stability. CGJO has elevated computational efficiency and an attractive detection capability for discovering the most accurate solution. For composite functions F9, F10, F11 and F12, CGJO exhibits superior durability and stability for identifying an accurate solution. The various evaluation indicators and computational solutions of the CGJO are substantially greater than those of the GJO, which are superior to those of the WO, HO, SCSO, NRBO, BKA, L-SHADE, LSHADE-EpsSin, CMA-ES, GJO, RGJO and SGJO methods. CGJO can enhance algorithmic parallelism, tap population diversity, avoid premature convergence, expand the feature space, improve search efficiency and increase information capacity. CGJO is durable and reliable for identifying the ideal solution.

The ANOVA graph of each methodology is shown in Fig. 4. The standard deviation can directly and objectively exhibit stability and reliability. The comparatively low standard deviation reveals that the method not only has favourable strength and durability but also integrates detection and mining to obtain an exact or subaccurate solution. The standard deviation, the basis for ranking, is an accurate measure of optimization efficiency and stability. For the unimodal function F1, CGJO is sufficiently stable and durable to provide supplementary advantages and balances exploration and extraction to increase computational precision and yield the best solution. The CGJO has strong stability and the best ranking. For basic functions F2, F3, F4 and F5, the various evaluation indicators and computational solutions of the CGJO are superior to those of the WO, HO, SCSO, NRBO, BKA, L-SHADE, LSHADE-EpsSin, CMA-ES, GJO, RGJO and SGJO, and the CGJO can determine the exact global subsolution of the partial functions, which highlights that the CGJO exhibits excellent search efficiency to promote the optimization ability. The standard deviation and the ranking of CGJO are superior to those of WO, HO, SCSO, NRBO, BKA, L-SHADE, LSHADE-EpsSin, CMA-ES, GJO, RGJO and SGJO, which highlights that CGJO has remarkable reliability and superiority in determining the best solution. For hybrid functions F6, F7 and F8, the various evaluation indicators and computational solutions of the CGJO are substantially better than those of the GJO. The standard deviations and rankings of the CGJO are relatively good, and the CGJO has great reliability and dependability. For composite functions F9, F10, F11 and F12, the CGJO not only exhibits great stability and reliability to supervise exploration and extraction and strengthen the optimization performance but also utilizes the diploid mechanism to encode the golden jackal individual and determine the exact solution. The CGJO method exhibits outstanding detection capability and optimization efficiency for identifying the most accurate solution. Compared with those of the GJO, the computational solutions of the CGJO have changed significantly. The standard deviation of CGJO is relatively better than that of WO, HO, SCSO, NRBO, BKA, L-SHADE, LSHADE-EpsSin, CMA-ES, GJO, RGJO and SGJO. CGJO uses an efficient search mechanism

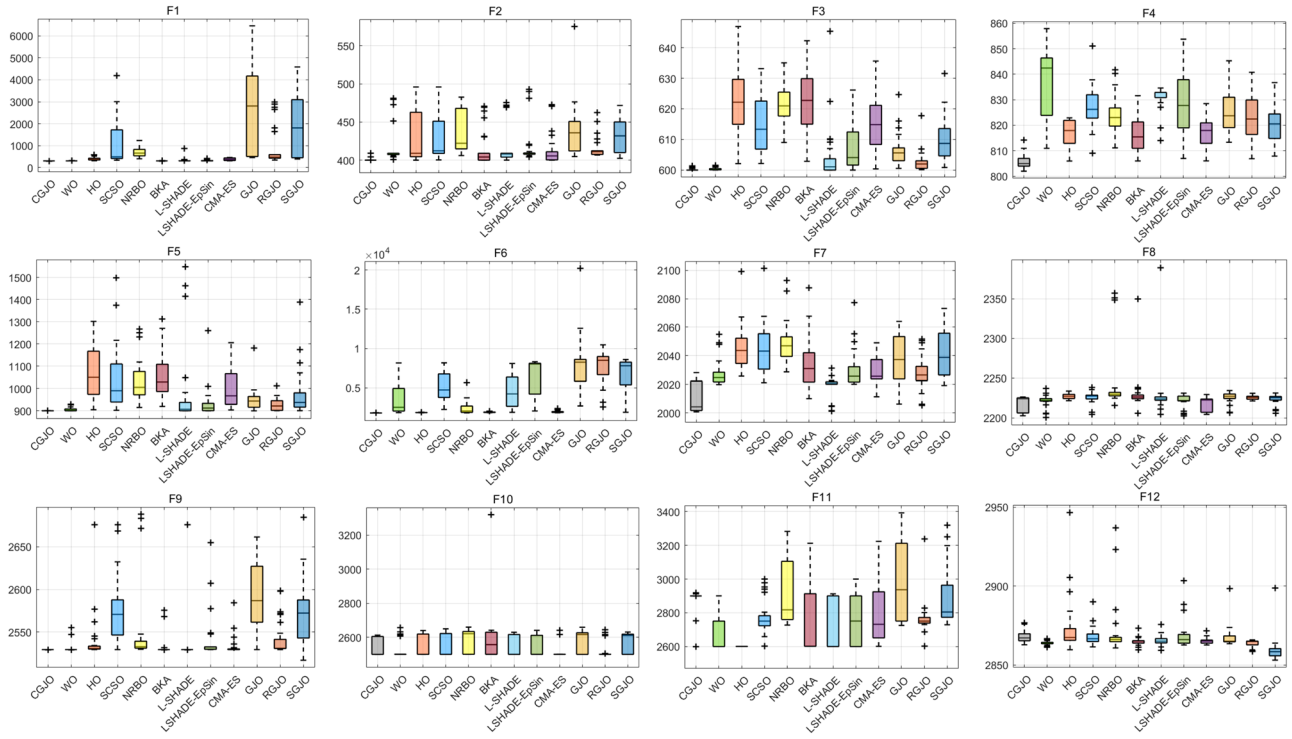

Fig. 4. ANOVAs of each methodology.

and stability to acquire accurate values. CGJO employs the diploid's two-dimensional properties to renew the jackal position and maximize the detection efficiency. CGJO not only combines exploration and extraction to broaden the optimization area and enrich the information capacity but also exhibits good stability and durability to prevent early convergence and identify accurate solutions.

CGJO for engineering design

To demonstrate dependability, CGJO is implemented to accomplish ten engineering designs: cantilever beam[44], three-bar truss[45], tubular column[46], piston lever[47], tension/compression spring[48] and gear train[49].

Cantilever beam

The main goal is to mitigate the ultimate beam's poundage, as shown in Fig. 5. There are five constraints, and a constant thickness is maintained ($t = 2/3$). The structure is as follows:

Consider

$$x = [x_1\ x_2\ x_3\ x_4\ x_5] \tag{32}$$

Minimize

$$f(x) = 0.6224(x_1 + x_2 + x_3 + x_4 + x_5) \tag{33}$$

Subject to

$$g(x) = \frac{61}{x_1^3} + \frac{37}{x_2^3} + \frac{19}{x_3^3} + \frac{7}{x_4^3} + \frac{1}{x_5^3} \leq 1 \tag{34}$$

Variable range

$$0.01 \leq x_1, x_2, x_3, x_4, x_5 \leq 100 \tag{35}$$

The statistical values of the cantilever beam are outlined in Table 5. The CGJO method exhibits remarkable robustness and durability in identifying the most significant decision variables and the smallest values. The statistical significance of CGJO outweighs those of other methodologies, which highlights that CGJO has good optimization efficiency and convergence precision.

Three-bar truss

The primary intention is to mitigate the ultimate truss's poundage, as portrayed in Fig. 6. There are two constraints: sections A_1 and A_2. The structure is as follows:

Consider

$$x = [x_1\ x_2] = [A_1\ A_2] \tag{36}$$

Minimize

$$f(x) = (2\sqrt{2}x_1 + x_2) \times l \tag{37}$$

Subject to

$$g_1(x) = \frac{\sqrt{2}x_1 + x_2}{\sqrt{2}x_1^2 + 2x_1x_2}P - \sigma \leq 0 \tag{38}$$

$$g_2(x) = \frac{x_2}{\sqrt{2}x_2 + 2x_1x_2}P - \sigma \leq 0 \tag{39}$$

$$g_3(x) = \frac{1}{\sqrt{2}x_2 + x_1}P - \sigma \leq 0 \tag{40}$$

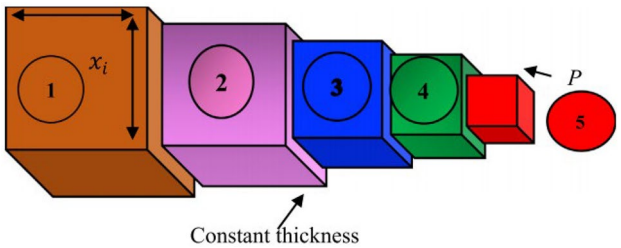

Fig. 5. Cantilever beam.

Algorithm	Optimal variable					Optimal cost
	x_1	x_2	x_3	x_4	x_5	
SCSO[3]	6.0164	5.3060	4.4935	3.5059	2.1516	1.3399524
CSO[3]	6.7628	5.1583	5.6537	2.9279	1.8854	1.3970239
GWO[3]	6.0103	5.3557	4.4827	3.5022	2.1248	1.3400590
GSA[3]	5.6052	4.9553	5.6619	3.1959	3.2026	1.4115575
PSO[3]	6.0040	5.2950	4.4915	3.5125	2.1710	1.3399830
BWO[3]	6.2094	6.2094	6.2094	6.2094	6.2094	1.9373625
KOA[50]	6.016	5.3092	4.4943	3.5015	2.1527	1.339956
FLA[50]	5.5907	5.5357	4.3654	3.83	2.3748	1.353859
COA[50]	6.5562	5.412	4.516	3.168	2.0082	1.351601
GTO[50]	6.0237	5.3041	4.488	3.5046	2.1534	1.33996
RUN[50]	6.0155	5.3088	4.4933	3.5041	2.1520	1.339957
WOA[50]	5.7240	5.5860	4.6935	3.3631	2.1942	1.345389
DO[50]	6.0220	5.3091	4.4932	3.4980	2.1515	1.339958
POA[50]	6.0157	5.3088	4.4981	3.4977	2.1534	1.339957
CSA[51]	6.0089	5.3049	4.5023	3.5077	2.1504	1.33999
MDWA[51]	5.9120	5.3783	4.4797	3.5480	2.1674	1.3372
FFA[51]	4.9987	4.9995	4.9937	5.7251	4.9983	1.6005
SCA[51]	6.2001	5.6914	4.3141	3.5473	1.9471	1.3506
AOA[52]	6.01513	5.02525468	4.25398594	3.312993832	2.037547058	1.3685
CGO[52]	6.01513	5.3093	4.495	3.50142	2.15278	1.33997
CGJO	6.0274	5.3386	4.4905	3.4837	2.1349	1.3356

Table 5. Statistical values of the cantilever beam.

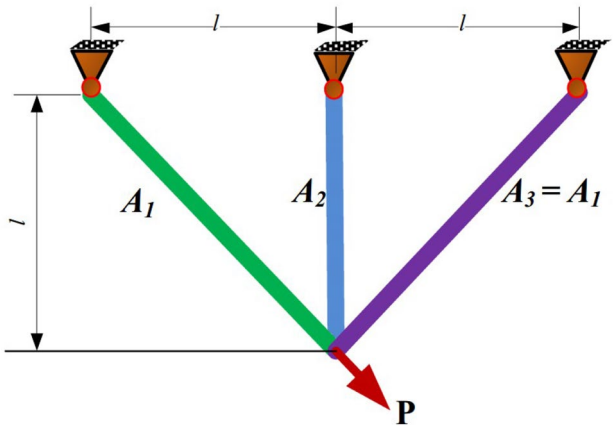

Fig. 6. Three-bar truss.

$$l = 100cm, \quad P = 2kN/cm^2, \quad \sigma = 2kN/cm^2 \tag{41}$$

Variable range

$$0 \le x_1, x_2 \le 1 \tag{42}$$

The statistical values of the three-bar truss are outlined in Table 6. The ideal outcomes of CGJO are superior to those of alternative methodologies. CGJO employs the two-dimensional properties of the diploid mechanism to inhibit premature convergence and acquire the most favourable statistical values, which highlights that CGJO has robust detection ability and reliability.

Tubular column

The primary intention is to mitigate the installation and material expenses, as portrayed in Fig. 7. There are two constraints: the average diameter (d) and breadth (t). The structure is as follows:

Consider

Algorithm	Optimal variable		Optimal cost
	A_1	A_2	
GA[53]	0.788915	0.407569	263.8958857
PSO[53]	0.788669	0.408265	263.8958434
ICA[53]	0.788625	0.408389	263.8958452
GWO[53]	0.788648	0.408325	263.8960063
WSA[53]	0.788683	0.408227	263.8958434
ESOA[54]	0.788192	0.409618	263.896
DE[54]	0.788675	0.408248	263.896
QANA[54]	0.788675	0.408248	263.895
MPEDE[54]	0.78924889	0.40662803	263.896
LSHADE[55]	0.785249	0.410335	263.8915
WOA[55]	0.78860276	0.408453070	263.8958
TEO[55]	0.7886618	0.4082831	263.8958
HGSO [55]	0.778254	0.440528	264.1762
HGS[55]	0.7884562	0.40886831	263.8959
AO-TSA[56]	0.790512	0.403105	263.9010
TSA[56]	0.797520	0.387339	264.3067
BO[56]	0.792187	0.398517	263.9159
GMO[57]	0.7886775	0.4082415	263.8958434
KABC[57]	0.7886	0.4084	263.8959
DMMFO[57]	0.788687421	0.408213541	263.8958435
CGJO	0.78192	0.42682	263.88416

Table 6. Statistical values of the three-bar truss.

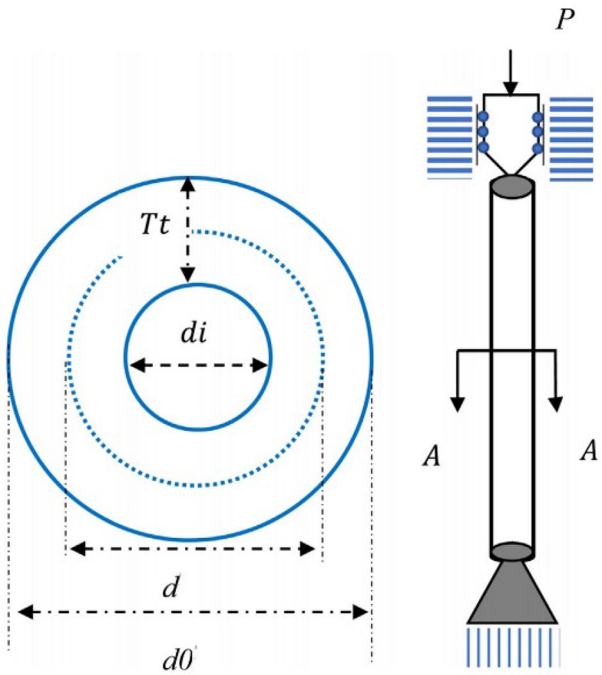

Fig. 7. Tubular column.

$$x = [x_1\ x_2] = [d\ t] \tag{43}$$

Minimize

$$f(x) = 9.82x_1x_2 + 2x_1 \tag{44}$$

Subject to

$$g_1(x) = \frac{P}{\pi x_1 x_2 \sigma_y} - 1 \leq 0 \tag{45}$$

$$g_2(x) = \frac{8PL^2}{\pi^3 E x_1 x_2 (x_1^2 + x_2^2)} - 1 \leq 0 \tag{46}$$

$$g_3(x) = \frac{2.0}{x_1} - 1 \leq 0 \tag{47}$$

$$g_4(x) = \frac{x_1}{14} - 1 \leq 0 \tag{48}$$

$$g_5(x) = \frac{0.2}{x_2 - 1} \leq 0 \tag{49}$$

$$g_6(x) = \frac{x_2}{0.8} - 1 \leq 0 \tag{50}$$

$$\sigma_y = 500 kgf / cm^2, \quad E = 0.85 \times 10^6 kgf / cm^2, \quad P = 2500 kgf, \quad L = 250 cm \tag{51}$$

Variable range

$$2 \leq x_1 \leq 14, \quad 0.2 \leq x_2 \leq 0.8 \tag{52}$$

The statistical values of the tubular column design are outlined in Table 7. The selection factors and expense of CGJO are superior to those of alternative methodologies. CGJO promotes algorithmic parallelism and increases population diversity to increase convergence efficiency, highlighting that CGJO is an efficient and predictable approach.

Piston lever

The primary intention is to mitigate the level and recognize the portions, as portrayed in Fig. 8. There are four constraints: H, B, X and D. The structure is as follows:

Consider

Algorithm	Optimal variable		Optimal cost
	d	*t*	
CSA[46]	5.451163397	0.291965509	26.531364472
MFPA[58]	5.4512	0.29197	26.49995
AGQPSO[59]	5.451156	0.29196	26.531328
FPA[60]	5.45116	0.291965	26.49948
KH[61]	5.451278	0.291957	26.5314
BOA[61]	5.448426	0.292463	26.512782
HFBOA[61]	5.451157	0.291966	26.499503
EM[62]	5.452383	0.29190	26.53380
HEM[62]	5.451083	0.29199	26.53227
KOA[50]	5.4512	0.2920	26.499497
FLA[50]	5.4801	0.2905	26.563266
COA[50]	5.4511	0.2920	26.501823
GTO[50]	5.4512	0.2920	26.499497
RUN[50]	5.4512	0.2920	26.499497
GWO[50]	5.4511	0.2920	26.499770
SMA[50]	5.4512	0.2920	26.499538
DO[50]	5.4512	0.2920	26.499497
POA[50]	5.4512	0.2920	26.499497
FA[52]	N/A	N/A	26.52
AOS[52]	N/A	N/A	26.5313783
CGJO	5.4532	0.2919	25.5615

Table 7. Statistical values of the tubular column design.

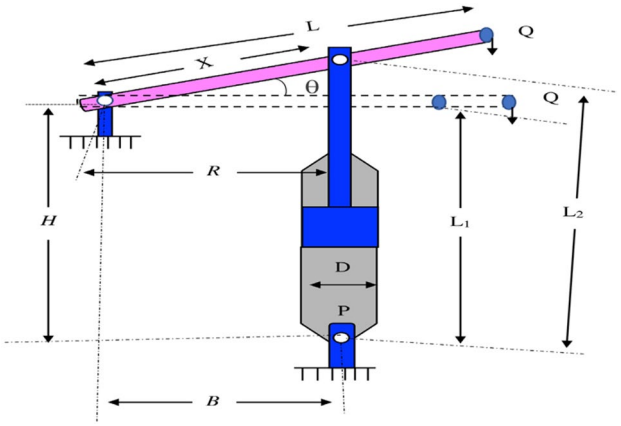

Fig. 8. Piston lever.

$$x = [x_1\ x_2\ x_3\ x_4] = [H\ B\ D\ X] \tag{53}$$

Minimize

$$f(x) = \frac{1}{4}\pi x_3^2(L_2 - L_1) \tag{54}$$

Subject to

$$g_1(x) = QL\cos\theta - RF \leq 0 \tag{55}$$

$$g_2(x) = Q(L - x_4) - M_{\max} \leq 0 \tag{56}$$

$$g_3(x) = \frac{6}{5} \times (L_2 - L_1) - L_1 \leq 0 \tag{57}$$

$$g_4(x) = \frac{x_3}{2} - x_2 \leq 0 \tag{58}$$

$$R = \frac{|-x_4(x_4\sin\theta + x_1) + x_1(x_2 - x_4\cos\theta)|}{\sqrt{(x_4 - x_2)^2 + x_1^2}} \tag{59}$$

$$F = \frac{\pi P x_3^2}{4} \tag{60}$$

$$L_1 = \sqrt{(x_4 - x_2)^2 + x_1^2} \tag{61}$$

$$L_2 = \sqrt{(x_4\sin\theta + x_1)^2 + (x_2 - x_4\cos\theta)^2} \tag{62}$$

$$\theta{=}45^o,\ Q = 10000lbs,\ L = 240in,\ M_{\max} = 1.8 \times 10^6 lbs\ in,\ P = 1500psi \tag{63}$$

Variable range

$$0.05 \leq x_1, x_2, x_4 \leq 500, \quad 0.05 \leq x_3 \leq 120 \tag{64}$$

The statistical values of the piston lever are outlined in Table 8. The CGJO generates real and imaginary parts to renew the jackal position and broaden the feature space. The statistical values of the CGJO are significant and optimal, which highlights that the CGJO has strong reliability and superiority in determining the best value.

Tension/compression spring

The primary intention is to mitigate the ultimate spring's poundage, as portrayed in Fig. 9. There are three constraints: line thickness (d), average thickness (D) and reactive size (N). The structure is as follows:

Consider

Algorithm	Optimal variable				Optimal cost
	H	*B*	*X*	*D*	
PSO[63]	133.3	2.44	117.14	4.75	122
DE[63]	129.4	2.43	119.8	4.75	159
GA[63]	250	3.96	60.03	5.91	161
HPSO[63]	135.5	2.48	116.62	4.75	162
SCSO[3]	0.050	2.040	119.99	4.083	8.40901438899551
CSO[3]	0.050	2.399	85.68	4.0804	13.7094866557362
GWO[3]	0.060	2.0390	120	4.083	8.40908765909047
WAO[3]	0.099	2.057	118.4	4.112	9.05943208079399
SSA[3]	0.050	2.073	116.32	4.145	8.80243253777633
GSA[3]	497.49	500	60.041	2.215	168.094363238712
BWO[3]	12.364	12.801	172.02	3.074	95.9980864948937
GTO[47]	0.05	2.052859	119.6392	4.089713	8.41270
MFO[47]	0.05	2.041514	120	4.083365	8.412698
WOA[47]	0.051874	2.045915	119.9579	4.085849	8.449975
PDO[52]	0.05	0.144897318	120	4.11572157	4.602
DMOA[52]	0.05	0.125073578	120	4.116042166	4.695
AOA[52]	0.05	0.125073578	120	4.116042166	7.738
CPSOGSA[52]	500	500	120	2.578147082	4.6949
BBO[52]	129.4	2.43	119.8	4.75	4.6956
SCA[52]	0.05	0.144897318	120	4.11572157	4.6977
CGJO	0.05	0.154283913	120	4.105452537	4.5999

Table 8. Statistical values of the piston lever.

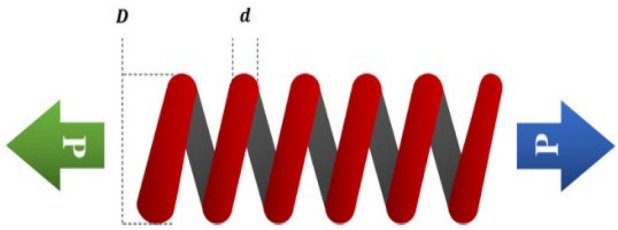

Fig. 9. Tension/compression spring.

$$x = [x_1\ x_2\ x_3] = [d\ D\ N] \tag{65}$$

Minimize

$$f(x) = (x_3 + 2)x_2x_1^2 \tag{66}$$

Subject to

$$g_1(x) = 1 - \frac{x_2^3 x_3}{71785x_1^4} \leq 0 \tag{67}$$

$$g_2(x) = \frac{4x_2^2 - x_1x_2}{12566(x_2x_1^3 - x_1^4)} + \frac{1}{5108x_1^2} \leq 0 \tag{68}$$

$$g_3(x) = 1 - \frac{140.45x_1}{x_2^2x_3} \leq 0 \tag{69}$$

$$g_4(x) = \frac{x_1 + x_2}{1.5} - 1 \leq 0 \tag{70}$$

Variable range

$$0.05 \leq x_1 \leq 2, \quad 0.25 \leq x_2 \leq 1.3, \quad 2 \leq x_3 \leq 15 \tag{71}$$

The statistical values of the tension/compression springs are outlined in Table 9. The CGJO implements the encoding technique to strengthen the discovery efficiency and increase the information capability. The CGJO has the finest variables and the lowest objective value, highlighting that the CGJO exhibits good durability and high calculation accuracy.

Gear train

The main goal is to optimize the tooth size and reduce the ultimate cost, as shown in Fig. 10. There are four constraints: n_A, n_B, n_C and n_D. The structure is as follows:

Consider

$$x = [x_1 \ x_2 \ x_3 \ x_4] = [n_A \ n_B \ n_C \ n_D] \tag{72}$$

Minimize

$$f(x) = \left(\frac{1}{6.931} - \frac{x_3 x_2}{x_1 x_4}\right)^2 \tag{73}$$

Variable range

Algorithm	Optimal variable			Optimal cost
	d	*D*	*N*	
SA[6]	0.0570	0.4953	6.2225	0.01321
GOA[6]	0.0516	0.3360	13.500	0.01389
HHO[6]	0.0570	0.4991	6.2180	0.01281
TSA[64]	0.051144	0.343751	12.0955	0.012674
MPA[64]	0.050178	0.341541	12.07349	0.012678321
TLBO[64]	0.050780	0.334779	12.72269	0.012709667
NGO[64]	0.0523593	0.372854	10.4093	0.012672
CSO[3]	0.0671	0.8482	2.4074	0.01682958
SCSO[3]	0.0500	0.3175	14.0200	0.012717020
CA[65]	0.05	0.317395	14.031795	0.012721
HPSO[65]	0.051706	0.357126	11.265083	0.0126652
CDE[65]	0.051609	0.354714	11.410831	0.0126702
AEO[65]	0.051897	0.361751	10.879842	0.0126662
ESOA[54]	0.05	0.317168	14.0715	0.01274345
QANA[54]	0.051926	0.362432	10.961632	0.01266625
MPEDE[54]	0.05956062	0.5767404	4.71717282	0.01374
NOA[66]	0.05169	0.35671	11.28932	0.0126652
GBO[66]	0.05187	0.36105	11.03921	0.0126658
GMO[57]	0.0514617	0.3512730	11.6154626	0.0126662
KABC[57]	0.0556	0.4575	7.148	0.013017
CGJO	0.050067	0.345798	11.806373	0.012664

Table 9. Statistical values of the tension/compression spring.

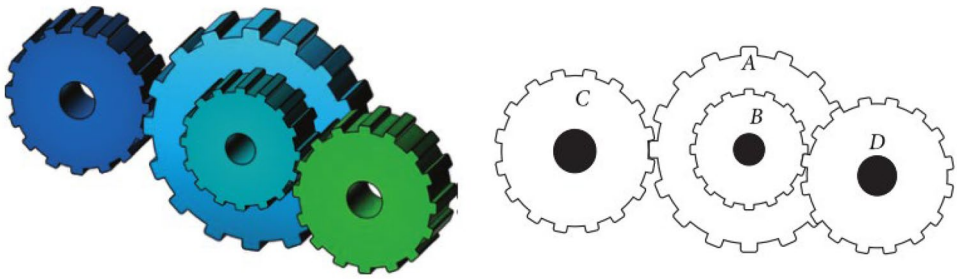

Fig. 10. Gear train.

$$12 \leq x_i \leq 60, \ \ i = 1, 2, ..., 4 \tag{74}$$

The statistical values of the gear train are outlined in Table 10. Compared with those of other methodologies, the objective variables of the CGJO have been extensively altered, which highlights that the CGJO exhibits remarkable reliability and adaptability to acquire an accurate solution.

Conclusions and future research

In this paper, CGJO is established to resolve the CEC 2022 test suite and six real-world engineering designs, and the purpose is to identify the global optimal exact solution of function optimization and the minimum cost of the engineering design. Complex-valued encoding employs the two-dimensional properties of the diploid methodology to describe one allele of a chromosome and renew the real and imaginary portions, which increases population diversity, restricts search stagnation, expands the exploration area, promotes information exchange, fosters collaboration efficiency and improves convergence accuracy. The CGJO has strong stability and robustness to overcome the low computational accuracy, premature convergence and poor solution efficiency. The CGJO combines GJO and complex-valued encoding to achieve complementary advantages and enhance computational efficiency. Therefore, CGJO not only exhibits fantastic stability and reliability to supervise exploration and extraction and strengthen the optimization performance but also utilizes the diploid mechanism to encode the golden jackal individual and determine the exact solution. The CGJO is compared with WO, HO, SCSO, NRBO, BKA, L-SHADE, LSHADE-EpsSin, CMA-ES, GJO, RGJO and SGJO. The experimental results reveal that the effectiveness and feasibility of CGJO are superior to those of other algorithms. CGJO has strong superiority and reliability to achieve a quicker convergence rate, greater computation precision, and greater stability and robustness.

The proposed CGJO has several limitations: (1) CGJO may face potential challenges in terms of computational complexity, mathematical theory analysis, astringency verification, and parameter selection. The calculation efficiency and solution accuracy may decrease. (2) When resolving complex, large-scale, high-dimensional multiobjective optimization problems, the CGJO may be limited and unable to balance exploration and exploitation to determine the superior convergence speed and calculation accuracy. (3) CGJO has strong stability and robustness for resolving the CEC 2022 test suite and six real-world engineering designs. However, the effectiveness and reliability of CGJO still need to be verified with more application datasets.

Future research on CGJO will focus on the following three aspects: (1) We will further study the mathematical theory, verify the algorithm astringency and select more effective control parameters through many experimental simulations. (2) We will introduce more effective search strategies (e.g., orthogonal opposition-based learning, the simplex method, the ranking-based mutation operator), unique encoding forms (e.g., quantum coding, discrete coding or binary coding), and hybrid swarm intelligence algorithms to achieve complementary advantages and avoid search stagnation, thereby increasing the overall convergence speed and calculation accuracy of the basic GJO. (3) According to the current situation of agricultural production in the Dabie Mountains in Anhui Province and the complex geographical environment of characteristic crops (e.g., Dendrobium, tea, rice, Chinese herbal

Algorithm	Optimal variable				Optimal cost
	n_A	n_B	n_C	n_D	
GA[53]	49	19	16	43	2.70E−12
PSO[53]	34	13	20	53	2.31E−11
ICA[53]	43	16	19	49	2.70E−12
BBO[53]	53	26	15	51	2.31E−11
NNA[53]	49	16	19	43	2.70E−12
GWO[53]	49	19	16	43	2.70E−12
WSA[53]	43	16	19	49	2.70E−12
KOA[50]	44	20	16	50	2.700857E−12
FLA[50]	44	16	20	49	2.700857E−12
COA[50]	23	14	12	48	9.92158E−10
RUN[50]	44	17	19	49	2.700857E−12
SMA[50]	52	30	13	53	2.307816E−11
DO[50]	49	16	19	44	2.700857E−12
POA[50]	44	17	19	49	2.700857E−12
PDO[52]	48	17	22	54	2.70E−12
DMOA[52]	49	19	16	43	2.70E−12
AOA[52]	49	19	19	54	2.70E−12
CPSOGSA[52]	55	16	16	43	2.31E−11
SSA[52]	49	19	19	49	2.70E−12
SCA[52]	49	19	34	49	2.700857E−12
CGJO	57	18	19	45	1.876542E−19

Table 10. Statistical values of the gear train design.

medicine), the CGJO can be used for intelligent detection and intelligent control of distinctive understorey crops. We will utilize underforest crop harvesting machinery and intelligence, underforest crop planting machinery and intelligence, precision plant protection equipment and intelligence to achieve underforest crop intelligent machinery and portable machinery and equipment.

Data availability

The datasets used and/or analysed during the current study available from the corresponding author on reasonable request. All data generated or analyzed during this study are included directly in the text of this submitted manuscript. There are no additional external files with datasets.

Received: 5 April 2024; Accepted: 19 August 2024
Published online: 23 August 2024

References

1. Han, M. *et al.* Walrus optimizer: A novel nature-inspired metaheuristic algorithm. *Expert Syst. Appl.* **239**, 122413 (2024).
2. Amiri, M. H., Mehrabi Hashjin, N., Montazeri, M., Mirjalili, S. & Khodadadi, N. Hippopotamus optimization algorithm: A novel nature-inspired optimization algorithm. *Sci. Rep.* **14**, 5032 (2024).
3. Seyyedabbasi, A. & Kiani, F. Sand Cat swarm optimization: A nature-inspired algorithm to solve global optimization problems. *Eng. Comput.* **39**, 2627–2651 (2023).
4. Sowmya, R., Premkumar, M. & Jangir, P. Newton-Raphson-based optimizer: A new population-based metaheuristic algorithm for continuous optimization problems. *Eng. Appl. Artif. Intell.* **128**, 107532 (2024).
5. Wang, J., Wang, W., Hu, X., Qiu, L. & Zang, H. Black-winged kite algorithm: a nature-inspired meta-heuristic for solving benchmark functions and engineering problems. *Artif. Intell. Rev.* **57**, 98 (2024).
6. Hashim, F. A., Houssein, E. H., Hussain, K., Mabrouk, M. S. & Al-Atabany, W. Honey Badger Algorithm: New metaheuristic algorithm for solving optimization problems. *Math. Comput. Simul.* **192**, 84–110 (2022).
7. Hashim, F. A. & Hussien, A. G. Snake Optimizer: A novel meta-heuristic optimization algorithm. *Knowl. Based Syst.* **242**, 108320 (2022).
8. Ajani, O. S., Kumar, A. & Mallipeddi, R. Covariance matrix adaptation evolution strategy based on correlated evolution paths with application to reinforcement learning. *Expert Syst. Appl.* **246**, 123289 (2024).
9. Chopra, N. & Ansari, M. M. Golden jackal optimization: A novel nature-inspired optimizer for engineering applications. *Expert Syst. Appl.* **198**, 116924 (2022).
10. Mohapatra, S. & Mohapatra, P. Fast random opposition-based learning Golden Jackal Optimization algorithm. *Knowl. Based Syst.* **275**, 110679 (2023).
11. Zhang, J., Zhang, G., Kong, M. & Zhang, T. Adaptive infinite impulse response system identification using an enhanced golden jackal optimization. *J. Supercomput.* https://doi.org/10.1007/s11227-023-05086-6 (2023).
12. Zhang, J., Zhang, G., Kong, M. & Zhang, T. SCGJO: A hybrid golden jackal optimization with a sine cosine algorithm for tackling multilevel thresholding image segmentation. *Multimed. Tools Appl.* https://doi.org/10.1007/s11042-023-15812-0 (2023).
13. Hanafi, A. V., Ghaffari, A., Rezaei, H., Valipour, A. & Arasteh, B. Intrusion detection in internet of things using improved binary golden jackal optimization algorithm and LSTM. *Clust. Comput.* https://doi.org/10.1007/s10586-023-04102-x (2023).
14. Ghandourah, E. *et al.* Performance prediction of aluminum and polycarbonate solar stills with air cavity using an optimized neural network model by golden jackal optimizer. *Case Stud. Therm. Eng.* **47**, 103055 (2023).
15. Wang, Z., Mo, Y. & Cui, M. An efficient multilevel threshold image segmentation method for COVID-19 imaging using Q-learning based golden jackal optimization. *J. Bionic Eng.* https://doi.org/10.1007/s42235-023-00391-5 (2023).
16. Das, H. *et al.* Feature selection using golden jackal optimization for software fault prediction. *Mathematics* **11**, 2438 (2023).
17. Snášel, V., Rizk-Allah, R. M. & Hassanien, A. E. Guided golden jackal optimization using elite-opposition strategy for efficient design of multi-objective engineering problems. *Neural Comput. Appl.* https://doi.org/10.1007/s00521-023-08850-0 (2023).
18. Houssein, E. H., Abdelkareem, D. A., Emam, M. M., Hameed, M. A. & Younan, M. An efficient image segmentation method for skin cancer imaging using improved golden jackal optimization algorithm. *Comput. Biol. Med.* **149**, 106075 (2022).
19. Zhang, K., Liu, Y., Mei, F., Sun, G. & Jin, J. IBGJO: Improved binary golden jackal optimization with chaotic tent map and cosine similarity for feature selection. *Entropy* **25**, 1128 (2023).
20. Lu, W., Shi, C., Fu, H. & Xu, Y. Fault diagnosis method for power transformers based on improved golden jackal optimization algorithm and random configuration network. *IEEE Access* https://doi.org/10.1109/ACCESS.2023.3265469 (2023).
21. Nanda Kumar, S. & Mohanty, N. K. Modified golden jackal optimization assisted adaptive fuzzy PIDF controller for virtual inertia control of micro grid with renewable energy. *Symmetry* **14**, 1946 (2022).
22. Wang, K., Gao, J., Kang, X. & Li, H. Improved tri-training method for identifying user abnormal behavior based on adaptive golden jackal algorithm. *AIP Adv.* https://doi.org/10.1063/5.0147299 (2023).
23. Yang, J. *et al.* Improved golden jackal optimization for optimal allocation and scheduling of wind turbine and electric vehicles parking lots in electrical distribution network using rosenbrock's direct rotation strategy. *Mathematics* **11**, 1415 (2023).
24. Najjar, I. R. *et al.* Prediction of tribological properties of alumina-coated, silver-reinforced copper nanocomposites using long short-term model combined with golden jackal optimization. *Lubricants* **10**, 277 (2022).
25. Mahdy, A., Hasanien, H. M., Turky, R. A. & Aleem, S. H. A. Modeling and optimal operation of hybrid wave energy and PV system feeding supercharging stations based on golden jackal optimal control strategy. *Energy* **263**, 125932 (2023).
26. Wang, Z., Mo, Y., Cui, M., Hu, J. & Lyu, Y. An improved golden jackal optimization for multilevel thresholding image segmentation. *Plos One* **18**, e0285211 (2023).
27. Wang, J. *et al.* An improved golden jackal optimization algorithm based on multi-strategy mixing for solving engineering optimization problems. *J. Bionic Eng.* **21**, 1092–1115 (2024).
28. Zhang, J., Zhang, G., Kong, M., Zhang, T. & Wang, D. Golden jackal optimization with lateral inhibition for image matching. *Multimed. Tools Appl.* https://doi.org/10.1007/s11042-024-18994-3 (2024).
29. Sundar Ganesh, C. S., Kumar, C., Premkumar, M. & Derebew, B. Enhancing photovoltaic parameter estimation: Integration of non-linear hunting and reinforcement learning strategies with golden jackal optimizer. *Sci. Rep.* **14**, 2756 (2024).
30. Bai, J., Khatir, S., Abualigah, L. & Wahab, M. A. Ameliorated Golden jackal optimization (AGJO) with enhanced movement and multi-angle position updating strategy for solving engineering problems. *Adv. Eng. Softw.* **194**, 103665 (2024).
31. Zhong, K., Xiao, F. & Gao, X. An efficient multi-objective approach based on golden jackal search for dynamic economic emission dispatch. *J. Bionic Eng.* https://doi.org/10.1007/s42235-024-00504-8 (2024).
32. Elhoseny, M., Abdel-salam, M. & El-Hasnony, I. M. An improved multi-strategy Golden Jackal algorithm for real world engineering problems. *Knowl. Based Syst.* **295**, 111725 (2024).
33. Alharthi, A. M. *et al.* Improving golden jackel optimization algorithm: An application of chemical data classification. *Chemom. Intell. Lab. Syst.* **250**, 105149 (2024).

34. Li, Y., Yu, Q., Wang, Z., Du, Z. & Jin, Z. An improved golden jackal optimization algorithm based on mixed strategies. *Mathematics* **12**, 1506 (2024).
35. Miao, F., Zhou, Y. & Luo, Q. Complex-valued encoding symbiotic organisms search algorithm for global optimization. *Knowl. Inf. Syst.* **58**, 209–248 (2019).
36. Zhang, J. *et al.* CWOA: A novel complex-valued encoding whale optimization algorithm. *Math. Comput. Simul.* **207**, 151–188 (2023).
37. Yan, Z., Zhang, J., Zeng, J. & Tang, J. Nature-inspired approach: An enhanced whale optimization algorithm for global optimization. *Math. Comput. Simul.* **185**, 17–46 (2021).
38. Yan, Z., Zhang, J. & Tang, J. Path planning for autonomous underwater vehicle based on an enhanced water wave optimization algorithm. *Math. Comput. Simul.* **181**, 192–241 (2021).
39. Huang, P. *et al.* Orthogonal opposition-based learning honey badger algorithm with differential evolution for global optimization and engineering design problems. *Alex. Eng. J.* **91**, 348–367 (2024).
40. Abdel-Basset, M., El-Shahat, D., Jameel, M. & Abouhawwash, M. Exponential distribution optimizer (EDO): A novel math-inspired algorithm for global optimization and engineering problems. *Artif. Intell. Rev.* **56**, 9329–9400 (2023).
41. Miao, F., Yao, L., Zhao, X. & Zheng, Y. Phasor symbiotic organisms search algorithm for global optimization. in *Intelligent Computing Theories and Application: 16th International Conference, ICIC 2020, Bari, Italy, October 2–5, 2020, Proceedings, Part I 16* 67–78 (Springer, 2020).
42. Miao, F., Wu, Y., Yan, G. & Si, X. A memory interaction quadratic interpolation whale optimization algorithm based on reverse information correction for high-dimensional feature selection. *Appl. Soft Comput.* **164**, 111979 (2024).
43. Miao, F. *et al.* Optimizing UAV path planning in maritime emergency transportation: A novel multi-strategy white shark optimizer. *J. Mar. Sci. Eng.* **12**, 1207 (2024).
44. Abualigah, L., Abd Elaziz, M., Sumari, P., Geem, Z. W. & Gandomi, A. H. Reptile search algorithm (RSA): A nature-inspired meta-heuristic optimizer. *Expert Syst. Appl.* **191**, 116158 (2022).
45. Emami, H. Stock exchange trading optimization algorithm: A human-inspired method for global optimization. *J. Supercomput.* **78**, 2125–2174 (2022).
46. Feng, Z., Niu, W. & Liu, S. Cooperation search algorithm: A novel metaheuristic evolutionary intelligence algorithm for numerical optimization and engineering optimization problems. *Appl. Soft Comput.* **98**, 106734 (2021).
47. Sadeeq, H. T. & Abdulazeez, A. M. Giant trevally optimizer (GTO): A novel metaheuristic algorithm for global optimization and challenging engineering problems. *IEEE Access* **10**, 121615–121640 (2022).
48. Zamani, H., Nadimi-Shahraki, M. H. & Gandomi, A. H. Starling murmuration optimizer: A novel bio-inspired algorithm for global and engineering optimization. *Comput. Methods Appl. Mech. Eng.* **392**, 114616 (2022).
49. Shen, Y., Zhang, C., Gharehchopogh, F. S. & Mirjalili, S. An improved whale optimization algorithm based on multi-population evolution for global optimization and engineering design problems. *Expert Syst. Appl.* **215**, 119269 (2023).
50. Abdel-Basset, M., Mohamed, R., Azeem, S. A. A., Jameel, M. & Abouhawwash, M. Kepler optimization algorithm: A new metaheuristic algorithm inspired by Kepler's laws of planetary motion. *Knowl. Based Syst.* **268**, 110454 (2023).
51. Rizk-Allah, R. M. & Hassanien, A. E. A movable damped wave algorithm for solving global optimization problems. *Evol. Intell.* **12**, 49–72 (2019).
52. Ezugwu, A. E., Agushaka, J. O., Abualigah, L., Mirjalili, S. & Gandomi, A. H. Prairie dog optimization algorithm. *Neural Comput. Appl.* **34**, 20017–20065 (2022).
53. Kaveh, A. & Eslamlou, A. D. Water strider algorithm: A new metaheuristic and applications. in *Structures* vol. 25, pp. 520–541 (Elsevier, 2020).
54. Chen, Z. *et al.* Egret swarm optimization algorithm: An evolutionary computation approach for model free optimization. *Biomimetics* **7**, 144 (2022).
55. Hashim, F. A., Mostafa, R. R., Hussien, A. G., Mirjalili, S. & Sallam, K. M. Fick's Law Algorithm: A physical law-based algorithm for numerical optimization. *Knowl. Based Syst.* **260**, 110146 (2023).
56. Akyol, S. A new hybrid method based on Aquila optimizer and tangent search algorithm for global optimization. *J. Ambient Intell. Humaniz. Comput.* **14**, 8045–8065 (2023).
57. Wu, H. *et al.* Wild geese migration optimization algorithm: A new meta-heuristic algorithm for solving inverse kinematics of robot. *Comput. Intell. Neurosci.* https://doi.org/10.1155/2022/5191758 (2022).
58. Meng, O. K., Pauline, O., Kiong, S. C., Wahab, H. A. & Jafferi, N. Application of modified flower pollination algorithm on mechanical engineering design problem. in *IOP conference series: materials science and engineering* vol. 165, pp. 012032 (IOP Publishing, 2017).
59. Kumar, N., Mahato, S. K. & Bhunia, A. K. A new QPSO based hybrid algorithm for constrained optimization problems via tournamenting process. *Soft Comput.* **24**, 11365–11379 (2020).
60. Nigdeli, S. M., Bekdaş, G. & Yang, X.-S. Application of the flower pollination algorithm in structural engineering. in *Metaheuristics and Optimization in Civil Engineering*, pp. 25–42 (2016).
61. Zhang, M., Wang, D. & Yang, J. Hybrid-flash butterfly optimization algorithm with logistic mapping for solving the engineering constrained optimization problems. *Entropy* **24**, 525 (2022).
62. Rocha, A. M. A. & Fernandes, E. M. Hybridizing the electromagnetism-like algorithm with descent search for solving engineering design problems. *Int. J. Comput. Math.* **86**, 1932–1946 (2009).
63. Kim, P. & Lee, J. An integrated method of particle swarm optimization and differential evolution. *J. Mech. Sci. Technol.* **23**, 426–434 (2009).
64. Dehghani, M., Hubálovskỳ, Š & Trojovskỳ, P. Northern goshawk optimization: A new swarm-based algorithm for solving optimization problems. *IEEE Access* **9**, 162059–162080 (2021).
65. Zhao, W., Wang, L. & Zhang, Z. Artificial ecosystem-based optimization: A novel nature-inspired meta-heuristic algorithm. *Neural Comput. Appl.* **32**, 9383–9425 (2020).
66. Abdel-Basset, M., Mohamed, R., Jameel, M. & Abouhawwash, M. Nutcracker optimizer: A novel nature-inspired metaheuristic algorithm for global optimization and engineering design problems. *Knowl. Based Syst.* **262**, 110248 (2023).

Acknowledgements

This work was partially funded by the Start-up Fund for Distinguished Scholars of West Anhui University under Grant Nos. WGKQ2022006, WGKQ2022050 and WGKQ2022052, the Scientific Research Projects of Universities in Anhui Province under Grant Nos. 2022AH051674 and 2022AH040241, the University Synergy Innovation Program of Anhui Province under Grant No. GXXT-2021-026, the Smart Agriculture and Forestry and Smart Equipment Scientific Research and Innovation Team (Anhui Undergrowth Crop Intelligent Equipment Engineering Research Center) under Grant No. 2022AH010091, the School-level quality engineering (school-enterprise cooperation development curriculum resource construction) under Grant No. wxxy2022101, the School-level Quality Engineering (Teaching and Research Project) under Grand No. wxxy2023079, the Open Fund of Anhui

Undergrowth Crop Intelligent Equipment Engineering Research Center under Grant No. AUCIEERC-2022-01. The authors would like to thank the editor and anonymous reviewers for their helpful comments and suggestions.

Author contributions

J.Z.: Conceptualization, Methodology, Software, Data curation, Formal analysis, Writing—original draft and Funding acquisition. G.Z.: Methodology, Resources, Writing—review & editing and Funding acquisition. M.K.: Conceptualization, Methodology, Writing—review & editing and Funding acquisition. T.Z.: Investigation, Validation, Writing—review & editing and Funding acquisition. D.W.: Project administration, Writing—review & editing and Funding acquisition.

Competing interests

The authors declare no competing interests.

Additional information

Correspondence and requests for materials should be addressed to G.Z.

Reprints and permissions information is available at www.nature.com/reprints.

Publisher's note Springer Nature remains neutral with regard to jurisdictional claims in published maps and institutional affiliations.